LARGE AND VERY LARGE SCALE STRUCTURES IN THE OUTER REGION OF AN ADVERSE PRESSURE GRADIENT TURBULENT BOUNDARY LAYER

Saeed Rahgozar
Department of Mechanical Engineering
Laval University
1065 avenue de la médecine, Quebec City, Quebec, G1V0A6, Canada
saeed.rahgozar.1@ulaval.ca

Yvan Maciel
Department of Mechanical Engineering
Laval University
1065 avenue de la médecine, Quebec City, Quebec, G1V0A6, Canada
Yvan.Maciel@gmc.ulaval.ca

ABSTRACT

Elongated regions of low and high momentum have been studied in the outer region of a turbulent boundary layer subjected to a strong adverse pressure gradient. Large sets of spanwise-streamwise instantaneous velocity fields are acquired by PIV (Particle Image Velocimetry) at three wall-normal positions (0.2δ, 0.5δ, 0.8δ) at three different streamwise locations in the adverse-pressure-gradient zone, from downstream of the strong suction peak up to detachment. Low- and high-speed regions are defined based on the fluctuating streamwise component of velocity. A pattern recognition method and a classification scheme are employed in order to obtain certain characteristics of the low- and high-speed *u*-structures. Like in the case of zero-pressure-gradient turbulent boundary layers, long meandering regions of low and high speed are observed in the outer region of the present flow. These structures are often longer than the 3δ streamwise length of our measurement planes and have dimensions that scale on boundary layer thickness. High- and low-speed *u*-structures are evenly spaced and their width is generally comparable to those previously reported for such structures in the overlap region of zero-pressure-gradient turbulent boundary layers. The results also show that the adverse pressure gradient not only reduces the frequency of appearance of streaky structures but also shortens them in the lower part of the outer region (at 0.2δ) while in the upper part (at 0.5δ and 0.8δ) their dimensions and arrangement seem to be unaffected by the pressure gradient.

INTRODUCTION

The existence of certain recurrent, organized and dynamically important structures in the turbulent flows has been generally accepted over the past several decades. The detection of the near-wall streaky structures with high- and low-speed regions aligned in the streamwise direction was one of the first clues to the existence of coherent structures within a turbulent boundary layer. Away from the wall in the outer region of the boundary layer, different types of dynamically important coherent structures have been observed by both numerical and experimental works. PIV measurements of Tomkins and Adrian (2003) and Ganapathisubramani et al. (2003) in the zero-pressure-gradient turbulent boundary layers (ZPG TBL) reveal that long regions of low momentum are the dominant large-scale motions in the upper buffer layer and in the logarithmic region.

Based on the premultiplied power spectra of streamwise velocity, Jiménez (1998) showed that structures with streamwise lengths of the order of $10-20$ boundary-layer thicknesses and containing a substantial fraction of the streamwise kinetic energy are present in the logarithmic region of wall-bounded flows. Kim and Adrian (1999) found that streamwise energetic modes with wavelengths reaching 12-14 radii exist in the outer layer of fully developed turbulent pipe flow at different Reynolds numbers. They suggest that these large structures may be a concatenation of hairpin packets. Hutchins and Marusic (2007) used hot-wire rake measurements to present evidence of very long meandering structures of positive and negative streamwise velocity fluctuation extending to over 20δ in length in the log and lower wake regions of a turbulent boundary layer. It was also mentioned by them that these superstructures, as they call them, maintain a footprint in the near-wall region.

In contrast to the situation in canonical wall flows, not much is known about the characteristics and behaviour of coherent structures in adverse-pressure-gradient (APG) turbulent boundary layers. Skote and Henningson (2002) noted that near-wall streaks vanish at separation. They also found that near-wall streaks are weaker and the spanwise spacing of the streaks in viscous unit is wider in their APG TBL flow.

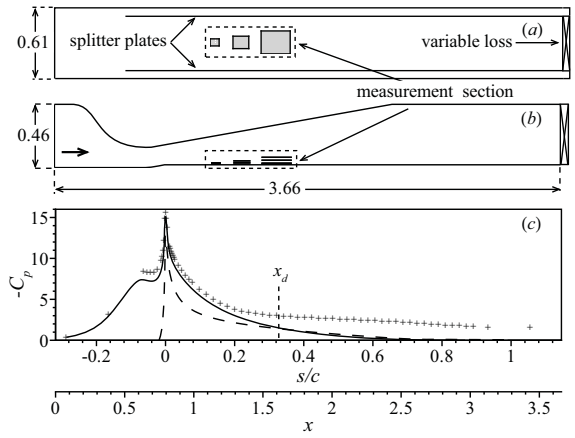

Figure 1. The experimental setup. (*a,b*) Respectively, top view and side view of the modified test section of the boundary-layer wind tunnel. (*c*) Pressure coefficient distribution along the floor of the test section: (+) measurement, − − NACA 2412 airfoil (chord of 2.5 m, $Re_c = 2.5\times10^6$, angle of attack of 18°), — potential flow calculation; $x_d = 1615$ mm is the position where $C_f = 0$. All dimensions in m.

Lee and Sung (2009) investigated the effect of APG on turbulent structures by carrying out direct numerical simulations of two equilibrium APG turbulent boundary layers. They found that the elongated low-momentum regions and hairpin packets are the dominant outer-layer structures. The present study focuses on the characteristics of large- and very large-scale structures in the form of low and high streamwise momentum in order to gain a better understanding of coherent structures in the outer region of APG turbulent boundary layers.

EXPERIMENT

The experiment was performed in the low-speed boundary-layer wind tunnel of the Laboratoire de Mécanique des Fluides at Laval University (figure 1*a,b*). A description of the setup can be found in Maciel et al. (2006). The setup was designed to reproduce external flow conditions typical of airfoils at high angle of attack with large trailing-edge flow detachment. Instantaneous velocity fields were acquired by PIV in streamwise-spanwise horizontal planes at three streamwise positions covering the APG region between the suction peak and the detachment point. At each streamwise position, three wall-normal measurements have been performed at 0.2δ, 0.5δ and 0.8δ with about 2000 velocity fields per plane (figure 1*a,b*). Another measurement with a horizontal plane was performed at a height of 0.1δ near the detachment zone ($x = 1477-1683$ mm) to be able to study in more detail the near-wall behaviour in that zone. The Reynolds number ($\mathrm{Re}_\theta = \theta U_e/\nu$) and the shape factor increase roughly from 5000 and 2 respectively, at the first streamwise location to 12000 and 3.6 respectively, at the third streamwise location (detachment zone). The field of view of each horizontal plane is approximately $3\delta \times 2.4\delta$. The current PIV measurements agree well with the results of Maciel et al. (2006).

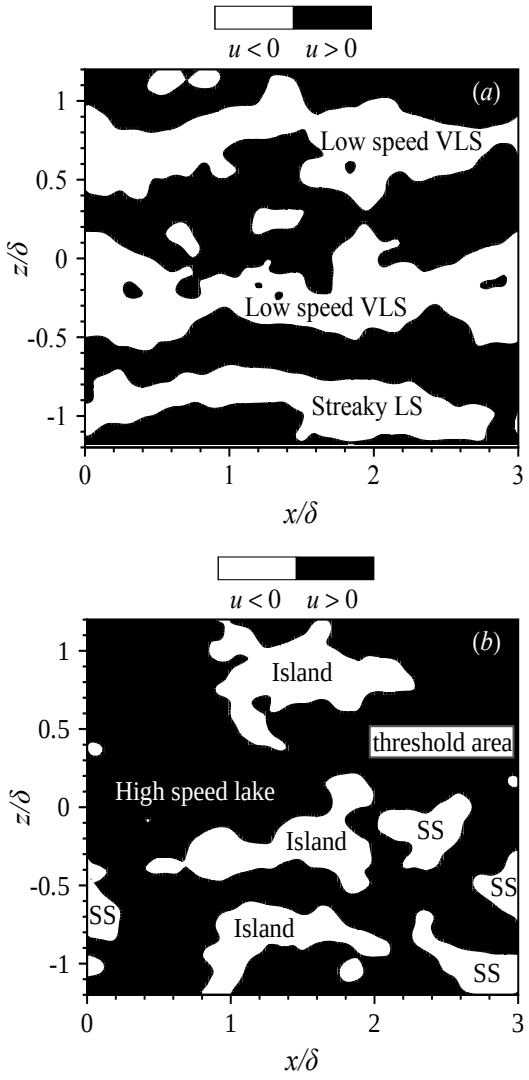

Figure 2. Sample fields. (*a*) An example of a streaky field. (*b*) An example of a field with a lake and islands; threshold area is represented with a rectangular surface.

DETECTION OF STRUCTURES

Low- and high-speed regions are defined based on the fluctuating streamwise component of velocity. A pattern recognition method is employed to detect *u*-structures. In order to be able to characterize them, the structures have been classified in three categories based on the area they cover: large scale (LS), small scale (SS) and lake. LSs are regions with the area larger than a chosen threshold; if the area is less than this threshold we call the region a SS. The threshold ($0.2\delta^2$) is obtained based on the large scale dimensions reported in previous studies (Tomkins and Adrian, 2003; del Álamo et al., 2006). Moreover, if an LS structure exceeds the streamwise borders of the measurement field on both sides, the structure is tagged as a very-large-scale structure (VLS) (figure 2*a*). Finally, in the case that there is just one very large region of low or high speed in the field, we call this region a lake of low or high speed respectively (figure 2*b*). Inside the low speed lakes, we always see islands of high speed and in the high-speed lakes, islands of low speed. So, a field contains

essentially low-speed (high-speed) islands if and only if it is a lake of high speed (low speed) (figure 2*b*). Furthermore, if a field does not contain a lake it usually contains streaky LS. Therefore, a field is streaky if and only if it is neither a lake of low speed nor a lake of high speed (figure 2*a*).

To summarize, VLS is a subset of streaky LSs; the latter and islands are the only two disjoint subsets of LSs. Finally, LSs, SSs and lakes are disjoint sets. Once the structures have been detected and classified, parameters of low- and high-speed u-structures such as frequency of appearance, length, width, distance-to-width ratio, length-to-width ratio and spanwise angle can be estimated.

RESULTS

The results are presented in three main sections. The first section discusses the frequency of appearance of the structures. Wall-normal and streamwise variations of the low- and high-speed LSs are studied in the following two sections respectively.

Frequency Of Appearance

Figure 3 shows the frequency of appearance of fields containing a lake or islands or streaky structures of low and high momentum in the first and third streamwise locations. It should be noted that, if we exclude the fields containing lakes, in 99% of the fields there are at least one LS region of low speed and one LS region of high speed (in average 2-3 of each) thus fields containing only SS of both high and low momentum are rare. With these considerations in mind, figure 3(*a*) shows that streaky fields are dominant at 0.2δ and 0.5δ at the first streamwise position. Even with significant differences in flow condition, the same behaviour exists at the second streamwise position (not shown). This agrees with several studies which support the existence of alternating zones of high- and low-speed fluid in the log and outer region of ZPG and APG TBL (Tomkins and Adrian, 2003; Hutchins and Marusic, 2007; Lee and Sung, 2009). In contrast, at 0.8δ low-speed islands are dominant. The dominance of the low-speed islands near the boundary-layer edge is consistent with the idea that turbulence forms bulges or ramp shapes in the outer region surrounded by higher-speed irrotational flow (Adrian et al., 2000).

Figure 3(*b*) presents the same information for the detachment zone. The frequency of appearance of the large-scale momentum structures is not comparable with the ones at the first and the second streamwise positions. In the lower part of the outer region ($y = 0.2\delta$), the islands of high speed (lakes of low speed) are dominant while at $y = 0.8\delta$, it is the islands of low speed (lakes of high speed) who are dominant. In the middle of the boundary layer ($y = 0.5\delta$), there is a balance between fields containing a lake or islands or streaky structures. Predominance of the high-speed islands near the wall could be explained by the dominance of Q4 events (sweeps) and the lack of Q2 events (ejections) that was observed in other APG TBLs (Simpson, 1991; Krogstad and Skåre, 1995). The region of maximum turbulence activity in a strong APG flow is in the middle of the boundary layer (Simpson, 1991; Krogstad and Skåre, 1995; Maciel et al., 2006) thus spots of energetic motion from the middle of the boundary layer may

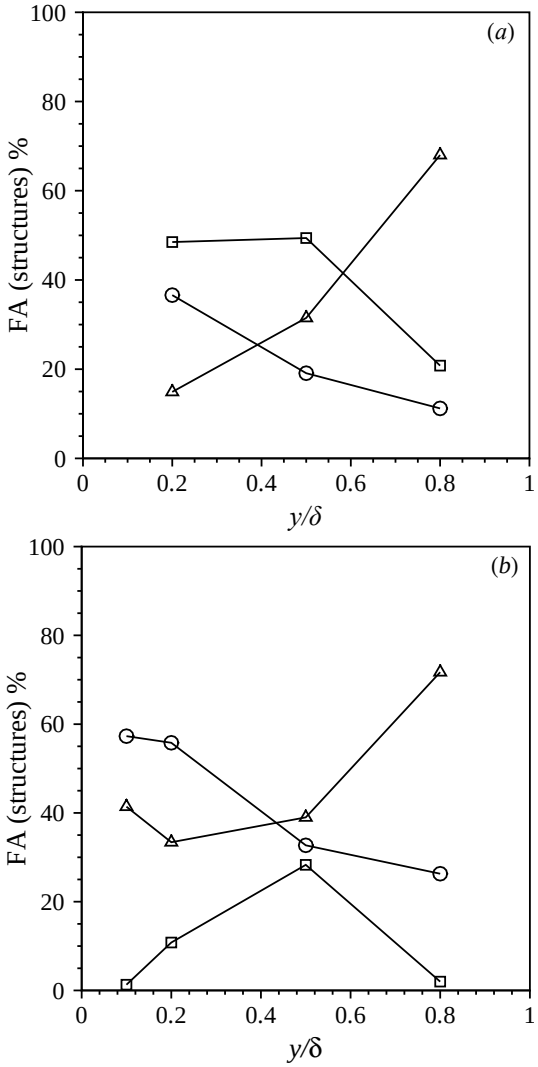

Figure 3. (*a*) The frequency of appearance (FA) of fields containing a lake or islands or streaky structures of low and high momentum at the first streamwise location, (*b*) Same as (*a*) but in the detachment zone: (□) streaky structures; (△) low-speed islands (high-speed lakes); (◯) low-speed lakes (high-speed islands); lines are for visual aid only.

move toward the wall into the inactive but big regions of low speed (low-speed lakes) as well as toward the boundary-layer edge into the large and often irrotational regions of high speed (high-speed lakes). In addition, the extinction of the streaky structures in the near-wall region of the separation zone, as it is implied by figure 3(*b*), is consistent with the studies which mentioned that near-wall streaks vanish at separation (Na and Moin, 1998; Skote and Henningson, 2002). Figure 3(*b*) also shows that in this large-defect boundary layer, streaky low- and high-speed regions tend to survive in the middle of the boundary layer ($y = 0.5\delta$). Although there are no significant differences between the frequency of appearance of lakes at the first and second streamwise positions, more lakes are observed at the detachment zone especially in the region closer to the wall. At all streamwise locations, more low-speed lakes have been observed in the lower part of the boundary layer,

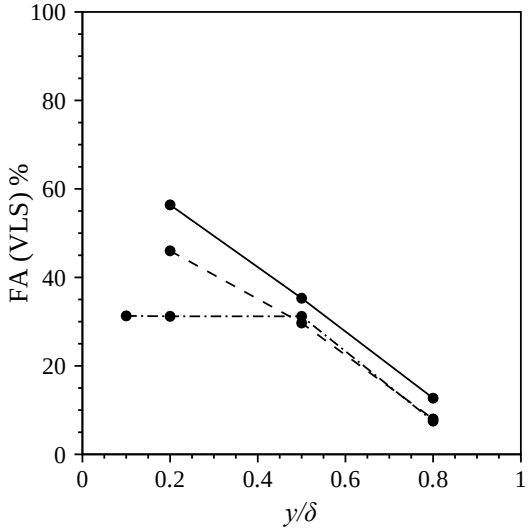

Figure 4. The frequency of appearance of low-speed VLS: —— first streamwise location; − − second streamwise location; −·− third streamwise location (detachment zone). Lines are for visual aid only.

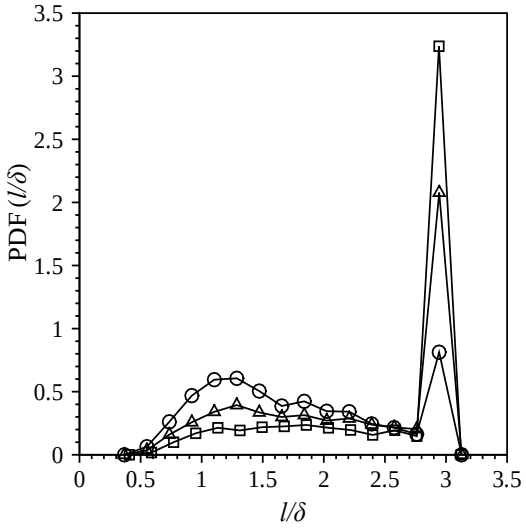

Figure 5. PDFs of the length of low-speed u-structures at the first streamwise location: (□) $y = 0.2\delta$; (△) $y = 0.5\delta$; (◯) $y = 0.8\delta$.

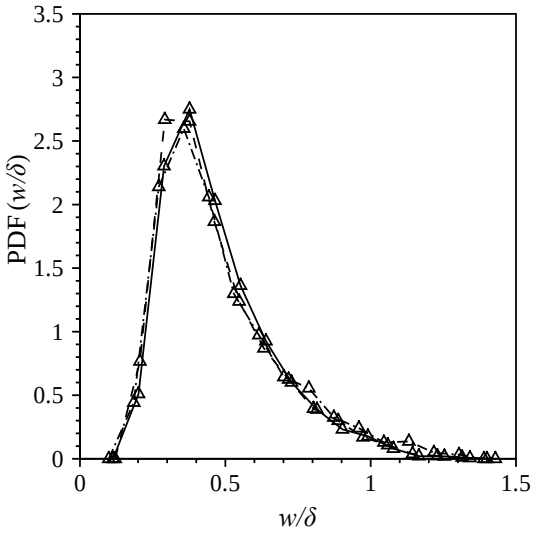

Figure 6. The PDFs of width of low-speed u-structures at $y = 0.5\delta$. Lines as in figure 4.

which can be related to the big inactive regions of low speed due to turbulent inactivity near the wall as we mentioned earlier. On the other hand, more high-speed lakes are seen near the boundary-layer edge which obviously is related to the existence of potential flow regions there. The growth of high-speed lakes near the detachment zone could be explained by the higher frequency of occurrence and persistence of Q4 motions (see Krogstad and Skåre, 1995), hence, a lake of high speed may sometimes be the result of the PIV plane cutting contiguous and large Q4 events.

Frequency of appearance of VLS (figure 4) is the percentage of LS which are VLS. This figure suggests that less VLS of low speed are located in the upper part of the boundary layer, which is consistent with what we already explained about the bulges and ramp shapes of turbulent zones. The VLS of high-speed regions have an opposite trend but with milder slope (not shown). It means that shorter high-speed regions are expected near the wall. Figure 4 also illustrates that closer to the wall, in the separation zone, we find less low-speed VLS than upstream. This reveals that the adverse pressure gradient shortens the low-speed regions and the same has been observed for high-speed regions. In the following sections, additional insights are gained by considering quantitative properties of the low- and high-speed regions.

Wall-normal Variations Of The LSs

In agreement with what we found from the frequency of appearance of the low-speed VLS, the probability density functions of the length of the low-speed LSs at the first (figure 5) and second streamwise locations (not shown) confirm the existence of shorter structures in the upper part of the boundary layer. In contrast, no considerable difference can be observed in the length of the high-speed LSs at different wall-normal positions (not shown). Moreover, two peaks can be easily recognized at heights 0.5δ and 0.8δ in figure 5. The peak at the maximum length ($l \approx 3\delta$), also present at all other wall-normal and streamwise positions, shows that the lengths of the low-speed LSs often exceed the size of the measurement planes which is consistent with several previous studies (Tomkins and Adrian, 2003; Hutchins and Marusic, 2007). The left peak reveals that structures with lengths of about 1δ to 1.5δ are also frequent in the upper part of the boundary layer. These may be related to the individual hairpin packets or vortex clusters that were detected by some researchers (Tomkins and Adrian, 2003; Ganapathisubramani et al., 2003; del Álamo et al., 2006).

The most probable width of both low-speed and high-speed LSs in all the planes is found to be between 0.3δ and 0.5δ and the mean value of width distributions is about 0.5δ (see figure 6). These values are comparable to those reported in ZPG TBL including Hutchins and Marusic (2007), 0.3δ to

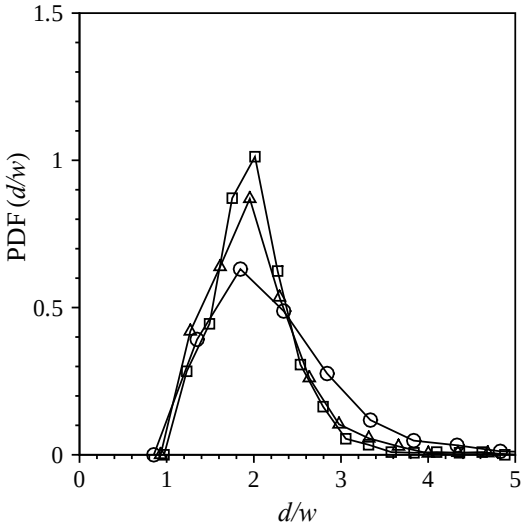

Figure 7. PDFs of distance-to-width of low-speed u-structures at the first streamwise location. Symbols as in figure 5 .

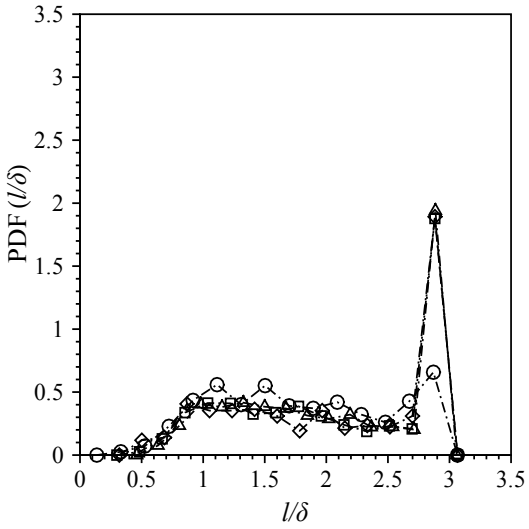

Figure 8. PDFs of the length of low-speed u-structures at the detachment zone. Symbols as in figure 5.

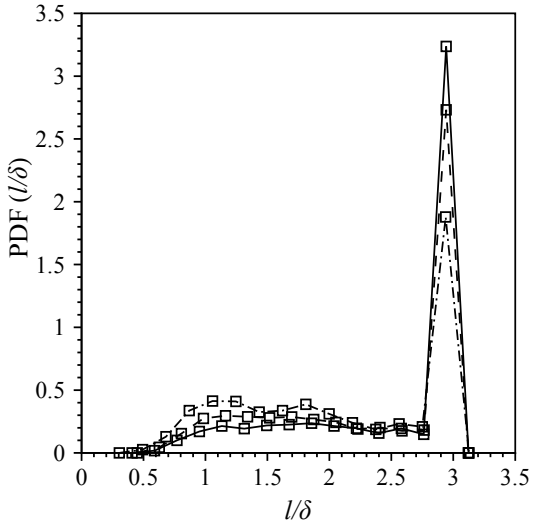

Figure 9. PDFs of the length of low-speed u-structures at $y = 0.2\delta$. Lines as in figure 4.

0.5δ; Tomkins and Adrian (2003), 0.1δ to 0.4δ. Lee and Sung (2009) found that the width of the low-momentum regions is about 0.4δ in their numerical APG TBL of milder pressure gradient and lower Reynolds number than in the present flow.

To find out how streaky are the LSs, the length-to-width ratio has been calculated. The most probable length-to-width ratio is found to be between 2 and 5 for all the planes but it is between 4 and 5 for the planes where streaky LSs are more frequent (see figure 3 for the frequency of appearance of the streaky LSs). This again confirms the streaky shape of the structures which are elongated in the streamwise direction.

Although the streaky structures are roughly aligned in the streamwise direction, the PDFs of the spanwise angle (ϕ) (not shown) of LSs reveal inclinations of up to 30° for both low speed and high speed while the most probable angle is about 0°.

The distance-to-width ratio indicates the arrangement of low-speed and high-speed LSs in the fields. Typical PDFs of d/w are shown in figure 7 in the case of low-speed regions. The peak of the PDFs is at about $d/w = 2$ which implies that low-speed and high-speed LSs are evenly spaced. Almost the same shape of the PDFs is observed at all streamwise and wall-normal planes for both low-speed and high-speed LSs.

The PDFs of the length of the low-speed LSs are shown in figure 8 for the detachment zone. The peaks of the PDFs at the maximum length are at the same value for $y = 0.1\delta$, 0.2δ and 0.5δ. The comparison between these PDFs and the ones at the first streamwise position (figure 5) reveals that although in the middle of the boundary layer ($y = 0.5\delta$) the peak value is comparable, near the wall ($y = 0.1\delta$ and 0.2δ) low-speed LSs are shorter at the detachment zone. This is consistent with what we found from the frequency of appearance of the VLSs. Moreover, the predominance of 1δ to 1.5δ long low-speed structures is reduced at the detachment zone.

On the other hand, the peaks of the PDFs of high-speed LSs (not shown) at the maximum length show a different level between the lower and upper parts of the boundary layer, i.e. shorter structures near the wall at $y = 0.1\delta$ and 0.2δ. Again, this result is consistent with the frequency of appearance of VLSs. The PDFs of length-to-width ratio of low- and high-speed LSs at the detachment zone (not shown), in agreement with the frequency of appearance of structures (figure 3*b*), support the fact that the structures in the middle of the boundary layer are streakier than the ones at other heights at the detachment zone.

Since the structures in the middle of the boundary layer are more streaky near detachment, less spanwise angle variation is expected at $y = 0.5\delta$. The PDFs of spanwise angle (not shown) confirm this point and moreover reveal that there are no distinguishable differences at the other heights.

Streamwise Variations Of The LSs

As the turbulent boundary layer undergoes deceleration, the low-speed LSs in the lower part of the outer region become

progressively shorter (figure 9). This is consistent with the results of Skote et al. (1998) and Krogstad and Skåre (1995). On the other hand, although the PDFs of high-speed LSs do not show distinguishable differences between the first and second streamwise positions, high-speed LSs are clearly shorter at the detachment zone (not shown), however, they all have similar width distributions. Furthermore, a comparison between the peaks of PDFs of low-speed LSs and high-speed LSs at the maximum length reveals that in the lower part of the outer region, high-speed LSs are generally shorter than low-speed ones.

Low-speed and high-speed LSs in the upper part of the outer region (planes at 0.5δ and 0.8δ) are characterized by surprisingly almost no streamwise variation. Figure 6 shows an example of this situation. The same similarity exists for the other parameters: length, length-to-width ratio, spanwise angle and distance-to-width ratio. As a result, it can be concluded that the APG only affects the large u-structures in the lower part of the outer region.

CONCLUSION

Large- and very large-scale structures in the form of elongated meandering regions of low and high streamwise momentum in the outer region of an adverse-pressure-gradient turbulent boundary layer have been investigated using PIV. Like in the case of zero-pressure-gradient turbulent boundary layers, long meandering streaky regions of low and high speed are observed in the outer region of the present flow. These structures have dimensions that scale on boundary-layer thickness and are often longer than our 3δ-long measurement planes. Their dimensions are generally comparable to those previously reported for such u-structures in the overlap region of zero-pressure-gradient turbulent boundary layers. It is however shown that the adverse pressure gradient shortens the streaky u-structures in the lower part of the outer region while in the upper part, the probability density functions of all the characteristic parameters of these structures are fairly similar at all streamwise locations. Their dimensions and arrangement seem therefore to be unaffected by the pressure gradient in the upper part of the boundary layer, but this is not to say that the streaky u-structures are completely insensitive to the pressure gradient since they appear much less frequently in the large-velocity-defect zone near detachment. The streaky structures are the most frequently encountered large u-structures in the lower and middle parts (at $y = 0.2\delta$ and $y = 0.5\delta$) of the outer region at the two most upstream locations of the present flow, locations where the boundary layer is subjected to a strong adverse pressure gradient but the velocity defect is still only moderately large. In the detachment zone, the predominant large u-structures in the lower part of the outer region, at 0.1δ and 0.2δ, are high-speed islands (non-streaky) inside low-speed lakes. Since the region of maximum turbulence activity in a strong adverse-pressure-gradient flow is in the middle of the boundary layer, spots of energetic motion from the middle of the boundary layer may move toward the wall into the inactive but big regions of low speed (low-speed lakes) that are predominant near detachment. Although in the large-velocity-defect case, large-scale u-structures are much less streaky in the lower part of the outer region than upstream, streaky u-structures continue to exist in the middle of the boundary layer, at 0.5δ. Moreover, as expected, streaky velocity fields are always rare near the edge of the boundary layer, where low-speed islands inside high-speed lakes are the most frequently encountered large u-structures. This is consistent with the idea that turbulence forms inclined bulges or ramp shapes in the outer region surrounded by higher-speed irrotational flow.

REFERENCES

Adrian, R. J., Meinhart, C. D., and Tomkins, C. D. (2000). Vortex organization in the outer region of the turbulent boundary layer. *J. Fluid Mech.*, 422:1–54.

del Álamo, J. C., Jiménez, J., Zandonade, P., and Moser, R. D. (2006). Self-similar vortex clusters in the turbulent logarithmic region. *J. Fluid Mech.*, 561:329–358.

Ganapathisubramani, B., Longmire, E. K., and Marusic, I. (2003). Characteristics of vortex packets in turbulent boundary layers. *J. Fluid Mech.*, 478:35–46.

Hutchins, N. and Marusic, I. (2007). Evidence of very long meandering features in the logarithmic region of turbulent boundary layers. *J. Fluid Mech.*, 579:1–28.

Jiménez, J. (1998). The largest structures in turbulent wall flows. In *CTR Ann. Res. Briefs, Stanford University*, pages 137–154.

Kim, K. C. and Adrian, R. J. (1999). Very large scale motions in the outer layer. *Phys. Fluids*, 11(02):417–422.

Krogstad, P. Å. and Skåre, P. E. (1995). Influence of a strong adverse pressure gradient on the turbulent structure in a boundary layer. *Phys. Fluids*, 7:2014–2024.

Lee, J. H. and Sung, H. J. (2009). Structures in turbulent boundary layers subjected to adverse pressure gradients. *J. Fluid Mech.*, 639:101–131.

Maciel, Y., Rossignol, K. S., and Lemay, J. (2006). A study of a turbulent boundary layer in stalled-airfoil-type flow conditions. *Exp. Fluids*, 41(4):573–590.

Na, Y. and Moin, P. (1998). Direct numerical simulation of separated turbulent boundary layer. *J. Fluid Mech.*, 374:379–405.

Simpson, R. L. (1991). The Structure of the Near-Wall Region of Two-Dimensional Turbulent Separated Flow. *Phil. Trans. R. Soc. Lond.: Physical and Engineering Sciences*, 336(1640):5–17.

Skote, M. and Henningson, D. S. (2002). Direct numerical simulation of separated turbulent boundary layer. *J. Fluid Mech.*, 471:107–136.

Skote, M., Henningson, D. S., and Henkes, R. A. W. M. (1998). Direct numerical simulation of self-similar turbulent boundary layers in adverse pressure gradients. *Flow turbul. combust.*, 60(1):47–85.

Tomkins, C. D. and Adrian, R. J. (2003). Spanwise structure and scale growth in turbulent boundary layers. *J. Fluid Mech.*, 490:37–74.